ON THE COMPUTATION OF VISCOUS FORCES NEAR THE MOVING CONTACT LINE

S. Afkhami *[1], S. Zaleski[2], S. Popinet[2], A. Guion[3], and J. Buongiorno[3]
[1]*New Jersey Institute of Technology, Newark, NJ, USA*
[2]*Institut Jean Le Rond d'Alembert, UPMC & CNRS-UMR 7190, Paris, FRANCE*
[3]*Massachusetts Institute of Technology, Cambridge, MA, USA*

Summary Here we present a numerical modeling of partially wetting plate withdrawn from a liquid reservoir at small capillary numbers in situations where a dynamic contact line at a certain height forms. We show that the main part of the dissipation on the plate arrises from the viscous friction near the contact line region. Previously, we showed in [J. Comp. Phys., 228:5370–5389, 2009] that the computed viscous dissipation on the plate depends on the mesh resolution. Here we explore the effects of viscosity ratio on the calculation of viscous friction near the contact line region. We use an adaptive flow solver to focus the computations on contact line region. We discuss the accuracy of the computations of frictional drag close to the contact line region when varying the mesh resolution and the viscosity ratio.

NUMERICAL MODEL

We consider a computational domain $0 \leq x, y \leq 1$, with fluid 1 occupying $y < 0.35$ and fluid 2, $y > 0.35$ (see Fig. 1(a)). We use GERRIS [2-4] to numerically solve the Navier-Stokes and continuity equations, $\rho D\mathbf{u}/Dt = -\nabla p + \nabla \cdot \left[\mu \left(\nabla \mathbf{u} + \nabla \mathbf{u}^{\top}\right)\right] + \gamma\kappa\delta_s\mathbf{n} + \rho\mathbf{g}$, $\nabla \cdot \mathbf{u} = 0$, respectively, where $D/Dt = \partial_t + \mathbf{u} \cdot \nabla$, $\rho = \rho_1 C + \rho_2(1 - C)$, and $\delta_s\mathbf{n} = \nabla C$. Here, $\mathbf{u}$ is the velocity field, p the pressure, ρ the density, μ the viscosity, γ the surface tension, κ the interface curvature, $\mathbf{n}$ the normal to the interface (pointing from fluid 1 to fluid 2), δ_s the delta function centered at the interface, $\mathbf{g}$ the gravitational acceleration, and C(= 1 in fluid 1 and 0 in fluid 2) the color function. The location of the interface is determined from where the density jumps in value and is updated according to $D\rho/Dt = (\partial_t + \mathbf{u} \cdot \nabla)\,\rho = 0$. We solve this equation using a volume of fluid interface tracking method [1,2]. We use a volume wighted averaging and a harmonic mean averaging method for the computation of the viscosity in an interfacial cell, $\mu = \mu_2 C + \mu_2(1 - C)$, $1/\mu = 1(\mu_2 C) + 1/(\mu_2(1 - C))$, respectively.

RESULTS AND DISCUSSIONS

Consider a solid plate ($x = 0$) withdrawn from a fluid reservoir, as illustrated in Fig. 1(a), with a velocity $V_s = 1$. We fix the capillary number, $Ca = \mu_1 V_s/\sigma = 0.01$, the Reynolds number, $Re = \rho_1 V_s L/\mu_1 = 1$ (L is the size of the computational domain), the capillary length, $l_c = \sqrt{\sigma/(\rho_1 g)} \approx 0.3$, the density ratio, $\rho_1/\rho_2 = 100$, and vary the viscosity ratio, μ_1/μ_2, the mesh resolution, with the maximum mesh size Δ, and the equilibrium contact angle θ_{eq}. The results are computed to the stationary state, $t \to \infty$.

Here we report on the computation of the shear rate near the contact line region to shed light on the nature of the contact line friction force. We vary the viscosity ratio as well as the contact angle to understand the effect of the surrounding fluid and the surface wetting on the viscous dissipation. In Fig. 1(b), we plot the shear rates along the solid boundary. First, we show that the results depend on the mesh size. As shown, the maximum shear rate near the contact line is significantly increased by only doubling the mesh resolution. We note that further mesh refinement will lead to logarithmic divergence of the shear rate. When the viscosity ratio is increased, it appears that the maximum shear rate at the contact line only increases slightly. However, the location of this maximum shear rate is changed noticeably when changing the viscosity ratio. Interestingly, changing the equilibrium contact angle appears to have an insignificant effect on the maximum shear rate at the contact line. In Fig. 1(c), we show that using a volume weighted averaging versus a harmonic mean averaging can shift the location of the maximum shear rate, but it has no significant effect on the value of the maximum shear rate near the contact line. Figure 2 illustrates the flow fields near the contact line, at stationary state, when varying the viscosity ratio and the equilibrium contact angle. The streamline plots show a major shift in the stagnation point near the contact line when varying the viscosity ratio; i.e. for $\mu_1/\mu_2 = 1$, it is on the interface, while for $\mu_1/\mu_2 = 50$, it is inside liquid 2. The plot also shows the split streamlines in liquid 2. We observe that the angle of the split streamline varies when varying the viscosity ratio and the equilibrium contact angle.

CONCLUSIONS

We study the dynamics of moving contact lines for fluids with a large viscosity contrast. We report on the computation of the shear rate exerted by the solid wall on the liquid near the contact line region, and compare the results when varying the mesh size, viscosity ratio, and the equilibrium contact angle. We show that the shear rate diverges with mesh refinement. Interestingly, changing the equilibrium contact has no significant effect on the maximum shear rate at the contact line. The results of the flow topology suggest that for high viscosity ratios, a stagnation point near the contact line resides in the bulk, while for low viscosity ratios it is on the interface. This mechanism can be responsible for the difference in the bending of the interface and the topology of the flow close to the contact line.

*Corresponding author. Email: shahriar.afkhami@njit.edu

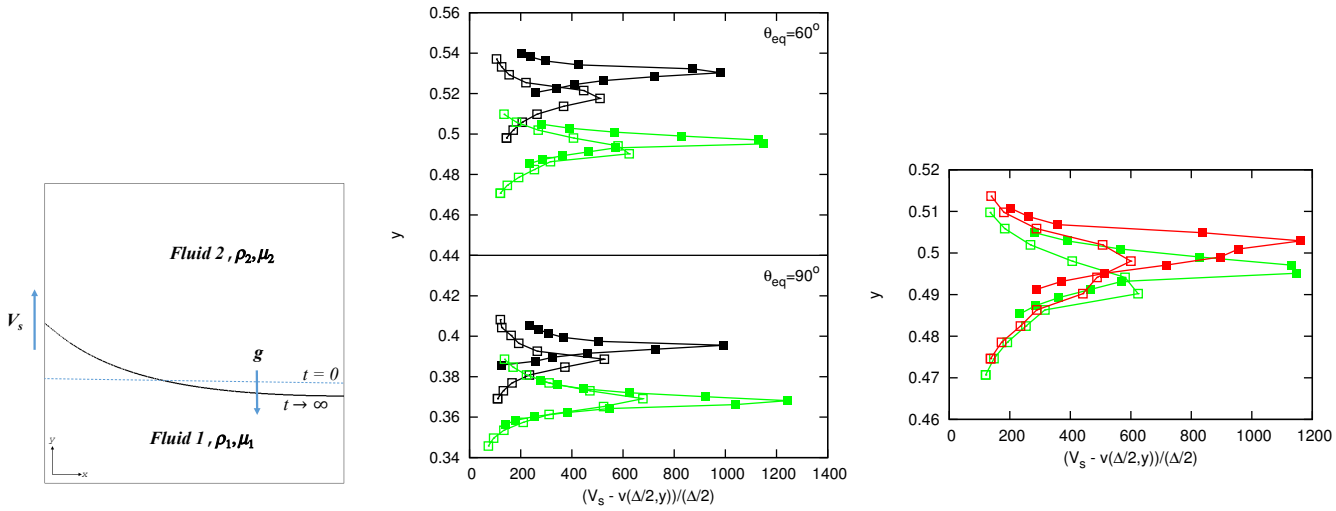

(a) (b) (c)

Figure 1: (a) Schematic of the withdrawing plate, initially at $t = 0$, and at the stationary state $t \to \infty$. (b) Stationary state shear rates at mesh resolutions $\Delta = 1/256$ (□) and $\Delta = 1/512$ (■), for $\mu_1/\mu_2 = 1$ (black) and $\mu_1/\mu_2 = 50$ (green). (c) Volume weighted averaging (red) versus harmonic mean averaging (green), $\mu_1/\mu_2 = 50$.

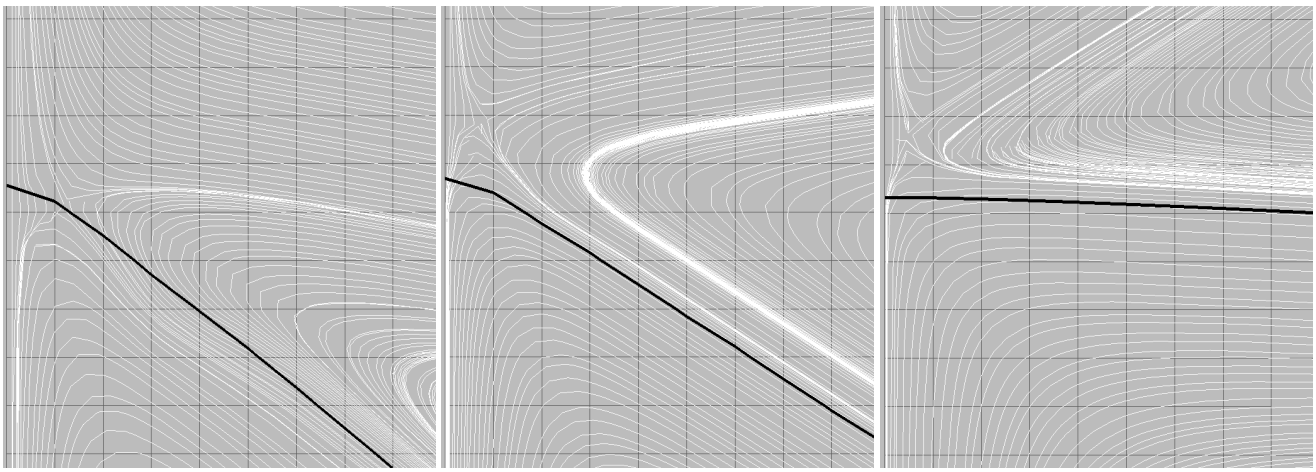

(a) (b) (c)

Figure 2: The flow fields near the contact line, at stationary state. The streamlines depict the slip of the contact line along the wall, as well as the parabolic flow field in fluid 1 and the split streamlines in liquid 2. (a) $\mu_1/\mu_2 = 1$, $\theta_{\text{eq}} = 60°$, (b) $\mu_1/\mu_2 = 50$, and $\theta_{\text{eq}} = 60°$, and (c) $\mu_1/\mu_2 = 50$, $\theta_{\text{eq}} = 90°$. $\Delta = 1/512$.

References

[1] Afkhami S., Zaleski S., Bussmann M.: A mesh-dependent model for applying dynamic contact angles to vof simulations. J. Comp. Phys., 228:5370–5389, 2009.

[2] Popinet S.: Gerris: a tree-based adaptive solver for the incompressible Euler equations in complex geometries. J. Comp. Phys., 190:572–600, 2003.

[3] Popinet S.: An accurate adaptive solver for surface-tension-driven interfacial flows. J. Comp. Phys., 228:5838–5866, 2009.

[4] Gerris Flow Solver, http://gfs.sourceforge.net.